

HYDRAULICS OF THE DEVELOPING FLOW REGION OF STEPPED SPILLWAYS. PART II: PRESSURE AND VELOCITY FIELDS

Gangfu Zhang ⁽¹⁾ and Hubert Chanson ⁽²⁾ (*)

⁽¹⁾ Ph.D. Research student, School of Civil Engineering, The University of Queensland, Brisbane, Australia

⁽²⁾ Professor in Hydraulic Engineering, The University of Queensland, School of Civil Engineering, Brisbane QLD 4072, Australia, Ph.: (61 7) 3365 4163, Fax: (61 7) 3365 4599, E-mail: h.chanson@uq.edu.au

(*) Corresponding author

Abstract: In skimming flow on a stepped spillway, the upstream flow motion is non-aerated and a turbulent boundary layer develops until the outer edge of the boundary layer interacts with the free-surface: that is, at the inception point of air entrainment. Herein new experiments were performed in the developing flow region on a large size 1V:1H stepped spillway model with step height $h = 0.10$ m. The flow properties in the developing flow region were carefully documented. In the developing boundary layer, the velocity distributions followed a $1/4.5^{\text{th}}$ power law at step edges. Detailed velocity and pressure measurements showed some rapid flow redistribution between step edges and above step cavities. The application of the momentum integral equation indicated an average friction factor of 0.18, close to the observed air-water flow friction factor of 0.23, suggesting that the spatially-averaged dimensionless shear stress was comparable in the developing flow and fully-aerated flow regions.

Keywords: Stepped spillways, Developing flow, Velocity distributions, Pressure distributions, Boundary shear stress, Energy dissipation.

INTRODUCTION

On an uncontrolled stepped spillway, the flow is accelerated by gravity. At the upstream end, a bottom boundary layer is generated by friction and develops in the flow direction. When the outer edge of the boundary layer becomes close to the free-surface, free-surface aeration takes place. Free-surface breakup and air entrainment occur because the turbulent shear stress is greater than the surface tension force per unit area resisting the interfacial breakup (Ervine and Falvey 1987, Chanson 2009, Bombardelli et al. 2011). Downstream of the inception point of free-surface aeration, the flow is fully-developed and rapid free-surface aeration is observed (Peyras et al. 1992, Chamani and Rajaratnam 1999, Chanson 2001). Recent prototype observations showed the presence of large surface scars upstream of the inception point (Chanson 2013) (Fig. 1). The scars were about 1.5 m to 1.7 m in size; the probability distribution function of surface scar production frequency was skewed with a preponderance of short frequencies relative to the mean; the median production frequency was 2.5 Hz (mode: 2.2 Hz) and the standard deviation was 0.87 Hz. Such surface scars were believed to be evidences of elongated hairpin vortices generated by boundary friction in the developing flow, stretched by the main strain field (Chanson 2013). Amador et al. (2006) performed a

ZHANG, G., and CHANSON, H. (2016). "Hydraulics of the Developing Flow Region of Stepped Spillways. II: Pressure and Velocity Fields." *Journal of Hydraulic Engineering*, ASCE, Vol. 142, No. 7, 9 pages (DOI:10.1061/(ASCE)HY.1943-7900.0001136) (ISSN 0733-9429).

characterisation of the developing flow using particle image velocimetry (PIV), although for a small range of laboratory flow conditions. The data showed maximum turbulence levels just behind the step edges, where the separation of the shear layer developed. Numerical simulations of these experiments suggested rapidly-varied velocity and pressure fields in the developing flow (Qian et al. 2009).

Herein velocity and pressure distributions, and energy dissipation were studied in the large-size steep stepped chute (1V:1H) under controlled flow conditions. The study aims to provide a new understanding of the hydrodynamics of the developing flow region on a steep stepped spillway model. The study outcomes provide a better characterisation of the flow resistance and highlight a number of challenges faced by the design engineers.

EXPERIMENTS AND INSTRUMENTATION

The experiments were conducted in a large-size stepped spillway model (1V:1H) (see Part I, in Zhang and Chanson 2016). The test section was 0.985 m wide and consisted of a broad-crested weir followed by twelve 0.1 m high flat steps. The water was fed from a large intake basin through a 2.8 m long side-wall convergent with a contraction ratio of 5.08:1, leading to a smooth and waveless inflow.

The discharge was deduced from detailed velocity and pressure measurements performed above the broad crested weir (see Part I, in Zhang and Chanson 2016). Clear-water flow depths were measured with a pointer-gauge on the channel centreline, as well as using photographic observations. The accuracy of the point gauges was ± 1 mm in the clear-water flow region. Clear-water pressure and velocity measurements were conducted using a Prandtl-Pitot tube ($\varnothing = 3.18$ mm) connected to an inclined manometer, with the tubes opened to the atmosphere. The error on the Prandtl-Pitot tube reading was less than 1 mm vertically. The longitudinal separation between the total and static tappings was taken into account, by repeating independently measurements at each location as illustrated in Figure 2. The vertical movement of the Prandtl-Pitot tube was controlled by a fine adjustment travelling mechanism. Further details were reported in Zhang and Chanson (see Part I, in Zhang and Chanson 2016).

Total and static pressure measurements were conducted in the clear water region upstream of the inception point of free-surface aeration for skimming flow conditions $d_c/h > 0.9$ where d_c is the critical flow depth: $d_c = (q^2/g)^{1/3}$, q is the water discharge per unit width, g is the gravity acceleration and h is the vertical step height. The data were recorded at selected longitudinal locations along the channel centreline using the Prandtl-Pitot tube for dimensionless discharges ranging from $d_c/h = 0.9$ to 1.7 (Table 1). The data were analysed in terms of velocity and pressure distributions, and energy dissipation in the developing flow region at each step edge and at several locations between adjacent step edges..

VELOCITY DISTRIBUTIONS IN THE DEVELOPING FLOW REGION

The velocity measurements showed that the water column consisted of a developing boundary layer with an ideal flow region above. The data indicated that the flow was accelerated by gravity in the downstream

ZHANG, G., and CHANSON, H. (2016). "Hydraulics of the Developing Flow Region of Stepped Spillways. II: Pressure and Velocity Fields." *Journal of Hydraulic Engineering*, ASCE, Vol. 142, No. 7, 9 pages (DOI:10.1061/(ASCE)HY.1943-7900.0001136) (ISSN 0733-9429).

direction. In the ideal flow region, the free-stream velocities matched theoretical predictions based upon the Bernoulli equation (Chanson 1999,2001). At each step edge, the boundary layer flow was characterised by a steep velocity gradient and the velocity profiles were best described by a power law (Chanson 2001, Amador et al. 2009, Meireles et al. 2012):

$$\frac{V_x}{V_o} = \left(\frac{y}{\delta} \right)^{1/N} \quad y < \delta \text{ at step edges (1)}$$

where V_x is the longitudinal velocity component, V_o is the free-stream velocity, y is the distance normal to the pseudo-bottom formed by the step edges, and δ is the boundary layer thickness defined in terms of 99% of the free-stream velocity. Typical velocity distributions are presented in Figure 3A. The best data fit yielded $N = 4.5$, with a normalised correlation coefficient $r = 0.97$. The value of N was close to that suggested by Chanson (2001) for a 1V:2H stepped model typical for embankment dams, but slightly different from $N = 3.0$ and 3.4 obtained by Amador et al. (2006) and Meireles et al. (2012) respectively. Figure 3B presents typical velocity contours for the entire flow between step edges 2 and 4, for $d_c/h = 1.5$. In Figure 3B, the measurement locations are marked with black dots, except at the free-surface where an ideal flow velocity was assumed. The data showed some rapid velocity redistributions in the skimming flow. Downstream of each step edge, some flow separation occurred and a shear layer developed. Following Pope (2000) and Amador et al. (2006), an upper bound of the shear layer may be: $y_{ub} = y_{0.9}$ where $y_{0.9}$ is the depth where $V_x = 0.9 \times V_o$. A typical evolution of the upper bound of the shear layer in the flow region surrounding step edge 3 is shown in Figure 4 for $d_c/h = 1.5$, where $k_s = h \times \cos\theta$ is the step cavity height and L_{cav} is the step cavity length: $L_{cav} = (h^2 + l^2)^{1/2}$. The data showed that the shear layer upper bound increased in the longitudinal direction downstream of the step edge and reached a maximum at approximately $x/L_{cav} = 0.8$, close to the finding of Amador (2005) (Fig. 4). The process was repeated at the next step edge and exhibited a wavy pattern over several steps. Note that the present study was unable to obtain a reliable estimate of the shear layer lower bound in the cavity flow region because of instrumentation limitations.

PRESSURE DISTRIBUTIONS IN THE DEVELOPING FLOW

The pressure distributions were derived from the piezometric head and water depth measurements. The data showed a rapidly varying pressure field in the developing flow region. Typical dimensionless pressure distributions are presented in Figures 5 and 6. In Figure 5, the hydrostatic pressure distribution is shown for comparison (red solid line). At step edges, the pressure profiles exhibited a linear shape in the ideal flow region immediately below the free-surface (Fig. 5C). The pressure gradient $\partial P/\partial y$ was often greater than hydrostatic, and tended to increase with increasing discharge, up to twice the hydrostatic pressure gradient for $d_c/h = 1.7$. The deviation from hydrostatic pressure distribution appeared to be a result of vertical flow accelerations linked to the free-surface curvature. Maximum pressures were typically observed in the mid- to lower-flow region, below which a pressure decrease was observed (Fig. 5C).

Pressure measurements immediately upstream and downstream of step edges showed distinctive patterns

ZHANG, G., and CHANSON, H. (2016). "Hydraulics of the Developing Flow Region of Stepped Spillways. II: Pressure and Velocity Fields." *Journal of Hydraulic Engineering*, ASCE, Vol. 142, No. 7, 9 pages (DOI:10.1061/(ASCE)HY.1943-7900.0001136) (ISSN 0733-9429).

(Fig. 5 & 6). Upstream of the step edge, the pressure gradient was consistently larger than hydrostatic throughout the entire water column; the findings were consistent with recent numerical data (Bombardelli 2014, *Pers. Comm.*), as well as horizontal step pressure data (Amador et al. 2009). The largest normalised bottom pressures were recorded for the smallest discharge ($d_c/h = 0.9$) (Fig. 5A). Immediately downstream of each step edge, flow separation took place and the dimensionless pressure was sub-atmospheric in the lower water column (Fig. 5D, 5E & 6). Such sub-atmospheric pressures were recorded by Toombes (2002) immediately below the step edges in nappe and transition flows, and by Sanchez-Juny et al. 2008 and Amador et al. (2009) in skimming flows. Maximum and minimum pressures appeared to be linked to flow stagnation upstream of and flow separation downstream of each step edge.

Figure 6 presents typical pressure contours above two step cavities. In Figure 6, the locations of pressure measurements are tagged with black dots, except at the free-surface where the pressure was atmospheric. The data showed a rapid redistribution of the pressure field in the flow direction (Fig. 5 & 6). The flow was characterised by alternating zones of positive and negative pressures. A large negative pressure zone was observed immediately downstream of step edge 3 in Figure 6, with a minimum pressure being below atmospheric. A positive pressure zone was observed next to the horizontal step face, linked to some interaction between the shear layer and the step face, with a change in streamline direction and flow stagnation immediately upstream of step edge 4 (Fig. 6). The occurrence of higher pressures at the lower edge of the cavity was consistent with numerical simulations (Qian et al. 2009, Bombardelli 2015, *Pers. Comm.*). Figure 6 also shows a few regions with a nearly-constant pressure gradient, implying that the streamlines were parallel despite the non-hydrostatic pressure distributions.

Present results demonstrated that the pressure distributions were not hydrostatic in the developing flow region on a stepped spillway, and the flow field was rapidly varied, with rapid longitudinal variations in both pressure and velocity distributions. The observations were consistent with the velocity data of Amador et al. (2006) and numerical modelling (Qian et al. 2009). A close examination of Figure 6 showed longitudinal variations in pressure profiles across step cavities: for example, the step cavity 2-3 was generally governed by positive pressures, while a negative pressure core was observed in step cavity 3-4. These observations may be attributed to the stepped geometry. The steps formed a series of expansions and contractions, forcing the flow to redistribute and leading to curved streamlines. The free-surface pattern was influenced by the combination of bottom geometry, slope and inflow conditions.

The present findings indicated that an improper stepped configuration might lead to the generation of significant free-surface curvatures and adverse negative pressures. An optimum design should seek to minimise any rapid flow variations to create a more uniform velocity and pressure field instead.

TOTAL HEAD, ENERGY DISSIPATION AND FLOW RESISTANCE

TOTAL HEAD DISTRIBUTIONS

In the developing flow region above the stepped chute, energy dissipation took place in the boundary layer

ZHANG, G., and CHANSON, H. (2016). "Hydraulics of the Developing Flow Region of Stepped Spillways. II: Pressure and Velocity Fields." *Journal of Hydraulic Engineering*, ASCE, Vol. 142, No. 7, 9 pages (DOI:10.1061/(ASCE)HY.1943-7900.0001136) (ISSN 0733-9429).

flow by means of viscous effect and turbulent interactions. The ideal fluid flow was little affected by the step macro-roughness, and the total head increased rapidly in the downstream direction according to ideal fluid flow calculations. Some energy was dissipated in the boundary layer, as indicated by the steep total head gradient in Figure 7A. The smallest values were recorded in the step cavity. Figure 7A shows a typical contour plot of dimensionless total head H_t/H_{dam} across two step cavities, where H_t and H_{dam} are the total head and dam height ($H_{dam} = 1.2$ m) respectively. At the free-surface, H_t was calculated using the Bernoulli equation. A yellow dashed line was drawn in Figure 7A to show the outer edge of the boundary layer for that flow rate.

The energy dissipation rate in the developing flow region was analysed based upon the total head measurements. At each step edge, the depth averaged specific energy was estimated as:

$$H_r = \frac{1}{d} \times \int_0^d (H_t - z_o) \times dy \quad (2)$$

where d is the flow depth, H_t is the total head and z_o is the step edge elevation above the datum. The normalised specific energy H_r/H_{max} along the stepped chute is shown in Figure 7B, where H_{max} is the maximum specific energy at any step edge along the spillway, L is the streamwise distance from the first step edge and L_i is the distance to the inception point of free-surface aeration. The present results showed a quasi-linear decrease in normalised specific energy as previously reported (Hunt and Kadavy 2010, Meireles et al. 2012). In Figure 7B, the present data are compared to an empirical correlation proposed by Meireles et al. (2012) for an ogee-crested spillway with a 1V:0.75H slope. The agreement between data and correlation was acceptable, although some data scatter was observed, possibly linked to the effects of free-surface curvature and by the distinct facilities.

BOUNDARY SHEAR STRESS

The flow resistance in a skimming flow is commonly estimated using the Darcy-Weisbach friction factor (Rajaratnam 1990, Chanson 2001), although its application to form losses is arguable (Chanson et al. 2002). The friction factor is essentially a dimensionless shear stress between the main streamflow and cavities, namely a spatially-averaged boundary shear stress along the pseudo-bottom since:

$$f = \frac{8 \times \overline{\tau_o}}{\rho \times V_o^2} \quad (3)$$

where f is the dimensionless boundary shear stress or Darcy-Weisbach friction factor, $\overline{\tau_o}$ is the (spatially-averaged) boundary shear stress and ρ is the fluid density. Herein the dimensionless boundary shear stress was estimated from the von Karman momentum integral equation applied to the developing boundary layer (Schlichting 1979):

$$\frac{\partial}{\partial x} (V_o^2 \times \delta_2) + V_o \times \delta_1 \times \frac{\partial V_o}{\partial x} = \frac{f_{MI}}{8} \times V_o^2 \quad (4)$$

where the subscript MI indicates calculations based upon the momentum integral equation (4), δ_1 is the

ZHANG, G., and CHANSON, H. (2016). "Hydraulics of the Developing Flow Region of Stepped Spillways. II: Pressure and Velocity Fields." *Journal of Hydraulic Engineering*, ASCE, Vol. 142, No. 7, 9 pages (DOI:10.1061/(ASCE)HY.1943-7900.0001136) (ISSN 0733-9429).

displacement thickness, δ_2 is the momentum thickness and x is the longitudinal coordinate. Equation (4) may be applied by both micro- and macro-roughness (Schlichting 1979) and does implicitly take into account the effects of gravity (Chanson 2014). The results are presented in dimensionless form in Figure 8 (red square symbols) and in a tabular form in Table 2. On average, the dimensionless boundary shear stress deduced from the momentum integral equation equalled: $f_{MI} \approx 0.182$ (Table 2). The result was close to the air-water flow friction factor estimates f_c obtained in the fully-developed flow region downstream of the inception point (Zhang and Chanson 2015, Fig. 8 hollow circle symbols). Amador (2005) and Meireles (2011) presented velocity measurements in the developing flow region of skimming flows: the application of the momentum integral equation gave on average $f_{MI} \approx 0.08$ to 0.12 (Table 2). Both the data of Meireles (2011) and Frizell et al. (2013) suggested a larger dimensionless shear stress f_{MI} for the largest step height h (Table 2), although these experiments were conducted for different relative step cavity roughness heights.

For completeness Amador (2005) reported time-averaged dimensionless tangential stresses $(\rho \times v_x \times v_y) / (\rho / 8 \times V_o^2)$ between 0 and 0.056 along the pseudo-bottom formed by the step edges in the developing flow region. His experimental observations yielded a spatially-averaged dimensionless shear stress $f_{xy} \approx 0.27$ over the entire step cavity. For comparison, Gonzalez and Chanson (2004) measured a spatially-averaged dimensionless shear stresses $f_{xy} \approx 0.34$, in the fully-developed air-water flow region (Table 2).

Lastly a gross estimate of the friction factor might be derived from the friction slope S_f ($S_f = -\partial H_t / \partial x$) assuming a fully-developed flow in a wide channel:

$$f_{Sf} = 8 \times S_f \times \left(\frac{d}{d_c} \right)^3 \quad (5)$$

where d is the flow depth. Equation (5) was applied in the developing flow region and the results are shown in Figure 8 (blue star symbols), although Equation (5) is only valid in fully-developed flows. The dimensionless shear stress data were close to those derived from Equation (5), despite the crude approximation.

Table 2 summarises the present data which are compared to previous studies. Altogether the experimental results were close, despite differences in stepped spillway geometry (slope, step height) and instrumentation. For completeness, note that Figure 8 regroups the present experimental data only.

CONCLUSION

In skimming flow on a stepped spillway, the developing flow region consists of a turbulent boundary layer and an ideal fluid flow above. Detailed pressure and velocity experiments were performed in the developing flow region on a large size 1V:1H stepped spillway model with step height $h = 0.10$ m. The experimental data showed a rapidly-varied flow motion. While the free-stream velocity accelerated in the downstream direction as predicted by the Bernoulli principle, the pressure distributions were not hydrostatic. Both velocity and pressure data indicated rapid flow redistributions between step edges and above each step

ZHANG, G., and CHANSON, H. (2016). "Hydraulics of the Developing Flow Region of Stepped Spillways. II: Pressure and Velocity Fields." *Journal of Hydraulic Engineering*, ASCE, Vol. 142, No. 7, 9 pages (DOI:10.1061/(ASCE)HY.1943-7900.0001136) (ISSN 0733-9429).

cavity. Close to the pseudo-bottom, a zone of positive pressures and another of negative pressures were governed respectively by flow stagnation and separation at each step edge.

The application of the von Karman momentum integral equation indicated an average friction factor of 0.18, close to and slightly lower than the observed air-water flow friction factor of 0.34. It is believed that this is the first study quantifying the boundary shear stress in both developing clear-water and fully-developed air-water flow regions, in the same facility for the same range of flow rates. The present finding suggested that the spatially-averaged dimensionless shear stress was comparable in the developing flow region and fully-aerated flow region of a stepped spillway, despite the rapidly-varied nature of the developing flow region.

The present findings highlighted the importance of physical modelling during the design process. An improper configuration might lead to the generation of significant free-surface curvatures and in turn adverse negative pressures.

ACKNOWLEDGEMENTS

The authors thank Professor Fabian Bombardelli (University of California Davis, USA), Professor Jorge Matos (IST Lisbon, Portugal) and Dr John Macintosh (Water Solutions, Australia) for their valuable advice. They acknowledge the technical assistance provided by Jason Van de Gevel and Stewart Matthews, the University of Queensland (Australia). The financial support of the Australian Research Council (Grant DP120100481) is acknowledged.

NOTATION

d water depth (m);

d_c critical flow depth (m);

F_* dimensionless discharge:

$$F_* = \frac{q}{\sqrt{g \times \sin\theta \times k_s^3}}$$

f (a) Darcy-Weisbach friction factor;

(b) dimensionless boundary shear stress;

f_e dimensionless shear stress in fully-developed air-water flows downstream of inception point of free-surface aeration;

f_{MI} dimensionless shear stress derived from von Karman momentum integral calculations;

f_{Sf} dimensionless shear stress derived from friction slope calculations;

f_{xy} spatially-averaged dimensionless Reynolds shear stress along a step cavity;

g gravity acceleration (m/s^2): $g = 9.80 m/s^2$ in Brisbane, Australia;

H_{dam} dam height (m);

H_r depth-averaged specific energy (m) on the stepped chute;

H_{max} maximum specific energy (m) at step edge;

ZHANG, G., and CHANSON, H. (2016). "Hydraulics of the Developing Flow Region of Stepped Spillways. II: Pressure and Velocity Fields." *Journal of Hydraulic Engineering*, ASCE, Vol. 142, No. 7, 9 pages (DOI:10.1061/(ASCE)HY.1943-7900.0001136) (ISSN 0733-9429).

H_t	total head (m);
h	vertical step height (m);
k_s	step roughness height (m): $k_s = h \times \cos\theta$;
L	longitudinal distance (m) positive downstream measured from step edge 1;
L_{cav}	step cavity length: $L_{cav} = (l^2 + h^2)^{1/2}$;
L_i	distance between step edge 1 and inception point of free-surface aeration;
l	horizontal step length (m);
P	pressure (Pa);
Q	water discharge (m^3/s);
q	water discharge per unit width (m^2/s);
S_f	friction slope;
V_x	longitudinal velocity component (m/s);
V_o	free-stream velocity (m/s);
v_x	longitudinal turbulent velocity fluctuation (m/s);
v_y	normal turbulent velocity fluctuation (m/s);
W	channel width (m);
x	longitudinal distance (m) positive downstream measured from step edge;
y	distance (m) normal to the invert, measured perpendicular to the pseudo-bottom formed by the step edges (on the stepped section);
y_{ub}	upper bound of the shear layer (m);
$y_{0.9}$	characteristic distance (m) where $V_x = 0.9 \times V_o$;
z_o	step edge elevation (m) above the datum;
δ	boundary layer thickness (m);
δ_1	displacement thickness (m);
δ_2	momentum thickness (m);
θ	angle between pseudo-bottom formed by step edges and horizontal;
ρ	water density (kg/m^3);
τ_o	boundary shear stress (Pa);
\emptyset	diameter (m);

Subscript

c	critical flow conditions;
i	inception point of free-surface aeration;
MI	momentum integral equation calculations;
Sf	friction slope calculations;

ZHANG, G., and CHANSON, H. (2016). "Hydraulics of the Developing Flow Region of Stepped Spillways. II: Pressure and Velocity Fields." *Journal of Hydraulic Engineering*, ASCE, Vol. 142, No. 7, 9 pages (DOI:10.1061/(ASCE)HY.1943-7900.0001136) (ISSN 0733-9429).

xy Reynolds stress calculations.

REFERENCES

- Amador, A (2005). "Comportamiento hidráulico de los aliviaderos escalonados en presas de hormigón compactado." *Ph.D. thesis*, Technical University of Catalonia (UPC), Barcelona, Spain (in Spanish).
- Amador, A., Sánchez-Juny, M. and Dolz, J. (2006). "Characterization of the nonaerated flow region in a stepped spillway by PIV." *Journal of Fluids Engineering*, Transactions of the ASME, Vol. 128, No. 6, pp. 1266-1273.
- Amador, A., Sánchez-Juny, M. and Dolz, J. (2009). "Developing flow region and pressure fluctuations on steeply sloping stepped spillways." *Journal of Hydraulic Engineering*, ASCE, Vol. 135, No. 12, pp. 1092-1100.
- Bombardelli, F.A., Meireles, I. and Matos, J. (2011). "Laboratory measurements and multi-block numerical simulations of the mean flow and turbulence in the non-aerated skimming flow region of steep stepped spillways." *Environmental Fluid Mechanics*, Vol. 11, No. 3, pp. 263-288.
- Chamani, M.R., and Rajaratnam, N. (1999). "Characteristics of Skimming Flow over Stepped Spillways." *Jl of Hyd. Engrg.*, ASCE, Vol. 125, No. 4, pp. 361-368.
- Chanson, H. (1999). "The hydraulics of open channel flow: an introduction." *Butterworth-Heinemann*, 1st edition, London, UK, 512 pages.
- Chanson, H. (2001). "The hydraulics of stepped chutes and spillways." *Balkema*, Lisse, The Netherlands, 418 pages.
- Chanson, H. (2009). "Turbulent air-water flows in hydraulic structures: dynamic similarity and scale effects." *Environmental Fluid Mechanics*, Vol. 9, No. 2, pp. 125-142 (DOI: 10.1007/s10652-008-9078-3).
- Chanson, H. (2013). "Interactions between a developing boundary layer and the free-surface on a stepped spillway: Hinze Dam spillway operation in January 2013." *Proc. 8th International Conference on Multiphase Flow ICMF 2013*, Jeju, Korea, 26-31 May, Gallery Session ICMF2013-005 (Video duration: 2:15).
- Chanson, H. (2014). "Applied Hydrodynamics: An Introduction." *CRC Press*, Taylor & Francis Group, Leiden, The Netherlands, 448 pages & 21 video movies.
- Chanson, H., Yasuda, Y., and Ohtsu, I. (2002). "Flow resistance in skimming flows and its modelling." *Canadian Journal of Civil Engineering*, Vol. 29, No. 6, pp. 809-819.
- Ervine, D.A., and Falvey, H.T. (1987). "Behaviour of turbulent water jets in the atmosphere and in plunge pools." *Proceedings of the Institution of Civil Engineers*, UK, Part 2, Mar., 83, pp. 295-314.
- Frizell, K. W., Renna, F. M., and Matos, J. (2013). "Cavitation potential of flow on stepped spillways." *Journal of Hydraulic Engineering*, ASCE, Vol. 139, No. 6, pp. 630-636.
- Gonzalez, C.A., and Chanson, H. (2004). "Interactions between cavity flow and main stream skimming flows: an experimental study." *Canadian Journal of Civil Engineering*, Vol. 31, No. 1, pp. 33-44.

- ZHANG, G., and CHANSON, H. (2016). "Hydraulics of the Developing Flow Region of Stepped Spillways. II: Pressure and Velocity Fields." *Journal of Hydraulic Engineering*, ASCE, Vol. 142, No. 7, 9 pages (DOI:10.1061/(ASCE)HY.1943-7900.0001136) (ISSN 0733-9429).
- Hunt, S. L., and Kadavy, K. C. (2010). "Energy dissipation on flat-sloped stepped spillways: part 1. upstream of the inception point." *Transactions ASABE*, Vol. 53, No. 1, pp. 103-109.
- Matos, J. (1999). "Emulsioneamento de ar e dissipação de energia do escoamento em descarregadores em degraus." ('Air entrainment and energy dissipation in flow over stepped spillways.') *Ph.D. thesis*, IST, Lisbon, Portugal (in Portuguese).
- Meireles, I. (2004). "Caracterização do escoamento deslizando sobre turbilhões e energia específica residual em descarregadores de cheias em degraus." ('Characterization of the skimming flow and residual energy in stepped spillways.') *M.Sc. thesis*, IST, Lisbon, Portugal (in Portuguese).
- Meireles, I. (2011). "Hydraulics of stepped chutes: experimental-numerical-theoretical study." *Ph.D. thesis*, Departamento de Engenharia Civil, Universidade de Aveiro, Portugal, 293 pages.
- Meireles, I., Renna, F., Matos, J., and Bombardelli, F.A. (2012). "Skimming, nonaerated flow on stepped spillways over roller compacted concrete dams." *Journal of Hydraulic Engineering*, ASCE, Vol. 138, No. 10, pp. 870-877.
- Peyras, L., Royet, P., and Degoutte, G. (1992). "Flow and energy dissipation over stepped gabion weirs." *Journal of Hydraulic Engineering*, ASCE, Vol. 118, No. 5, pp. 707-717.
- Pope, S., (2000). "Turbulent flows." *Cambridge University Press*, Cambridge, UK.
- Qian, Z.D., Hu, X.Q., Hu, W.X., and Amador, A. (2009). "Numerical simulation and analysis of water flow over stepped spillways." *Science in China Series E: Technological Sciences*, Vol. 52, No. 7, pp. 1958-1965.
- Rajaratnam, N. (1990). "Skimming flow in stepped spillways." *Journal of Hydraulic Engineering*, ASCE, Vol. 116, No. 4, pp. 587-591.
- Renna, F. (2004). "Caratterizzazione fenomenologica del moto di un fluido bifasico lungo scaricatori a gradini." ('Phenomenological characterization of two-phase flow along stepped spillways.') *Ph.D. thesis*, Politecnico di Bari, Cosenza, Italy (in Italian).
- Sánchez-Juny, M., Blade, E., and Dolz, J. (2008). "Analysis of pressures on a stepped spillway" *Journal of Hydraulic Research*, IAHR, Vol. 46, No. 3, pp. 410-414 (DOI: 10.3826/jhr.2008.3152).
- Schlichting, H. (1979). "Boundary Layer Theory." *McGraw-Hill*, New York, USA, 7th edition.
- Toombes, L. (2002). "Experimental study of air-water flow properties on low-gradient stepped cascades." *Ph.D. Thesis*, Dept. of Civil Engineering, University of Queensland, Australia.
- Zhang, G., and Chanson, H. (2015). "Broad-crested weir operation upstream of a steep stepped spillway." *Proc. 36th IAHR World Congress*, 28 June-3 July, The Hague, the Netherlands, Paper 79662, 11 pages (CD-ROM).
- Zhang, G., and Chanson, H. (2016). "Hydraulics of the Developing Flow Region of Stepped Spillways. I: Physical Modeling and Boundary Layer Development." *Journal of Hydraulic Engineering*, ASCE, Vol. 142, No. 7, 8 pages (DOI: 10.1061/(ASCE)HY.1943-7900.0001138) (ISSN 0733-9429).

ZHANG, G., and CHANSON, H. (2016). "Hydraulics of the Developing Flow Region of Stepped Spillways. II: Pressure and Velocity Fields." *Journal of Hydraulic Engineering*, ASCE, Vol. 142, No. 7, 9 pages (DOI:10.1061/(ASCE)HY.1943-7900.0001136) (ISSN 0733-9429).

Table 1 - Experimental flow conditions: stepped chute measurements (Present study)

Study location	Q (m ³ /s)	d _c /h	Location	Flow regime
Step edges	0.085 to 0.216	0.9 to 1.7	Step edges 2 to 8	Skimming flow
Step cavities	0.148 to 0.182	1.3 to 1.5	Step cavities 2 to 4	Skimming flow

Table 2 - Dimensionless boundary stress $f = \tau_o/(\rho/8 \times V_0^2)$ in skimming flows on stepped spillways - Average experimental results

Reference	θ (°)	W (m)	h (m)	Developing flow region			Aerated region	
				f _{MI} Momentum integral eq. (5)	f _{xy} Reynolds stress	f _{Sf} <i>Friction slope Eq. (6)</i>	f _{xy} Reynolds stress	f _e Friction slope Eq. (6)
Present study	45	1.0	0.10	0.182	--	<i>0.222</i>	--	0.345
Gonzalez & Chanson (2004)	15.9	1.0	0.10	--	--	--	0.34	0.15
Amador (2005)	51.3	0.5	0.05	0.124	0.27 ⁽³⁾	--	--	--
Meireles (2011) ⁽¹⁾	53.1	1.0	0.04 0.08	0.087 0.122	-- --	-- --	-- --	-- --
Frizell et al. (2013) ⁽²⁾	21.8 68.2	0.203	0.027 0.055 0.068 0.136	-- -- -- --	-- -- -- --	<i>0.089</i> <i>0.127</i> <i>0.160</i> <i>0.167</i>	-- -- -- --	-- -- -- --

Notes: f_e: dimensionless shear stress in fully-developed air-water flows downstream of inception point of free-surface aeration; f_{MI}: dimensionless shear stress derived from von Karman momentum integral calculations; f_{Sf}: dimensionless shear stress derived from friction slope calculations; f_{xy}: spatially-averaged dimensionless Reynolds shear stress along a step cavity; h: vertical step height; W: channel width; (--): data not available; *Italic*: approximate estimate, not strictly valid; ⁽¹⁾: experimental data by Matos (1999), Meireles (2004) and Renna (2004); ⁽²⁾: water tunnel data; ⁽³⁾: calculated by the authors based upon Amador's (2005) data.

ZHANG, G., and CHANSON, H. (2016). "Hydraulics of the Developing Flow Region of Stepped Spillways. II: Pressure and Velocity Fields." *Journal of Hydraulic Engineering*, ASCE, Vol. 142, No. 7, 9 pages (DOI:10.1061/(ASCE)HY.1943-7900.0001136) (ISSN 0733-9429).

LIST OF CAPTIONS

Fig. 1 - Fig. 1 - Hinze dam stepped spillway operation on 29 January 2013- Flow conditions: $q \sim 17 \text{ m}^2/\text{s}$, $d_c/h \sim 2.5$, $\theta = 51.3^\circ$ (1V:0.8H)

(A) View from downstream of the developing flow region and inception point of free-surface aeration

(B) View from upstream of the developing flow region and surface scars (red arrows)

Fig. 2 - Definition sketch of the stepped spillway model and Pitot tube positioning during flow measurements at step edges - Flow direction from left to right

Fig. 3 - Velocity distributions in the developing flow region of skimming flows on stepped spillway

(A) Dimensionless velocity distributions in the boundary layer at step edges (step edges 3 and 4)

(B) Dimensionless velocity contours V/V_c between step edges – Flow conditions: $d_c/h = 1.5$ – Flow direction from left to right

Fig. 4 - Upper bound of mixing layer in skimming flow, with flow direction from left to right and the origin at step edge 3 – Flow conditions: $d_c/h = 1.5$, $h = 0.10 \text{ m}$, $\theta = 45^\circ$ - Comparison with data of Amador (2005) for $d_c/h = 2.15$, $h = 0.05 \text{ m}$, $\theta = 51.3^\circ$

Fig. 5 - Dimensionless pressure distributions in skimming flows at locations immediately surrounding step edge 3

(A) $x/L_{cav} = -0.1$

(B) $x/L_{cav} = -0.05$

(C) Step edge 3: $x/L_{cav} = 0$

(D) $x/L_{cav} = +0.05$

(E) $x/L_{cav} = +0.1$

Fig. 6 - Dimensionless pressure field contour plot in skimming flow around step edge 3 - Flow conditions: $d_c/h = 1.5$, $h = 0.10 \text{ m}$, Flow direction from left to right

Fig. 7 - Total head distributions in the developing flow region of skimming flow

(A) Dimensionless total head distribution contours in skimming flows between step edges 2 and 4 for $d_c/h = 1.5$ - Yellow dashed line shows the outer edge of the boundary layer for that flow rate, Flow direction from left to right

(B) Longitudinal variation in dimensionless specific energy H_r/H_{max} in the developing flow region of skimming flows on a stepped spillway

Fig. 8 - Dimensionless boundary shear stress in the developing flow region of skimming flows on stepped spillways

ZHANG, G., and CHANSON, H. (2016). "Hydraulics of the Developing Flow Region of Stepped Spillways. II: Pressure and Velocity Fields." *Journal of Hydraulic Engineering*, ASCE, Vol. 142, No. 7, 9 pages (DOI:10.1061/(ASCE)HY.1943-7900.0001136) (ISSN 0733-9429).

Fig. 1 - Hinze dam stepped spillway operation on 29 January 2013- Flow conditions: $q \sim 17 \text{ m}^2/\text{s}$, $d_c/h \sim 2.5$, $\theta = 51.3^\circ$ (1V:0.8H)

(A) View from downstream of the developing flow region and inception point of free-surface aeration



(B) View from upstream of the developing flow region and surface scars (red arrows)



ZHANG, G., and CHANSON, H. (2016). "Hydraulics of the Developing Flow Region of Stepped Spillways. II: Pressure and Velocity Fields." *Journal of Hydraulic Engineering*, ASCE, Vol. 142, No. 7, 9 pages (DOI:10.1061/(ASCE)HY.1943-7900.0001136) (ISSN 0733-9429).

Fig. 2 - Definition sketch of the stepped spillway model and Pitot tube positioning during flow measurements at step edges - Flow direction from left to right

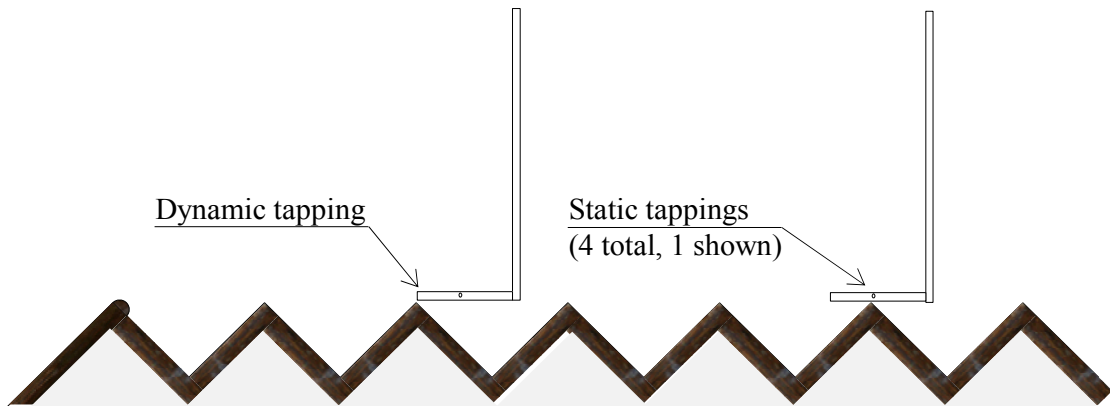
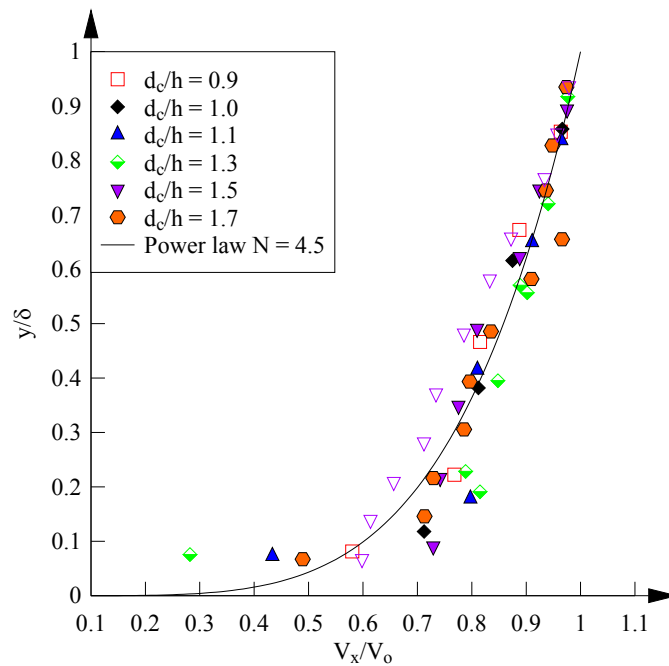
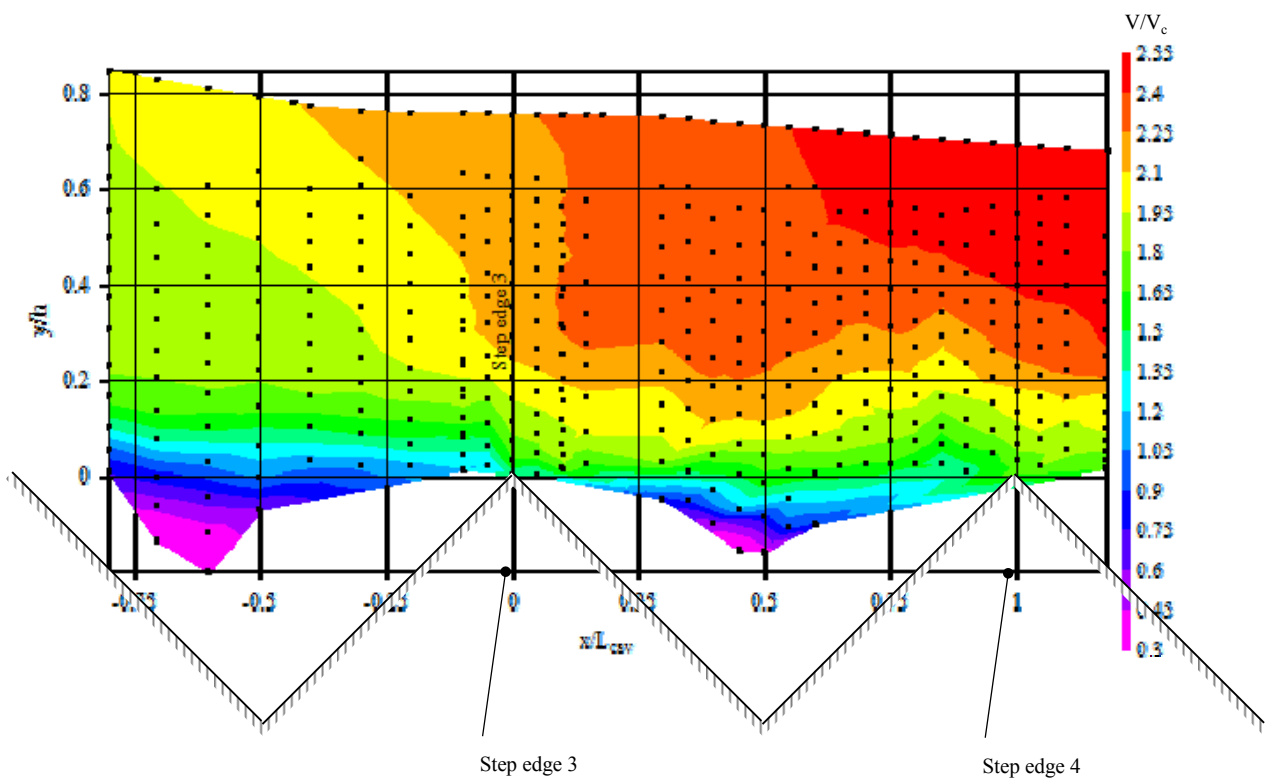


Fig. 3 - Velocity distributions in the developing flow region of skimming flows on stepped spillway
 (A) Dimensionless velocity distributions in the boundary layer at step edges (step edges 3 and 4)



(B) Dimensionless velocity contours V/V_c between step edges – Flow conditions: $d_c/h = 1.5$ – Flow direction from left to right



ZHANG, G., and CHANSON, H. (2016). "Hydraulics of the Developing Flow Region of Stepped Spillways. II: Pressure and Velocity Fields." *Journal of Hydraulic Engineering*, ASCE, Vol. 142, No. 7, 9 pages (DOI:10.1061/(ASCE)HY.1943-7900.0001136) (ISSN 0733-9429).

Fig. 4 - Upper bound of mixing layer in skimming flow, with flow direction from left to right and the origin at step edge 3 – Flow conditions: $d_c/h = 1.5$, $h = 0.10$ m, $\theta = 45^\circ$ - Comparison with data of Amador (2005) for $d_c/h = 2.15$, $h = 0.05$ m, $\theta = 51.3^\circ$

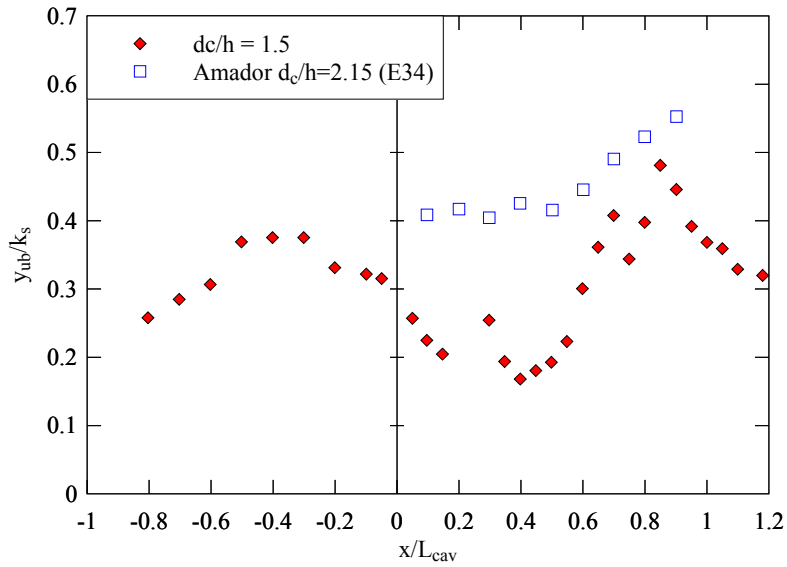
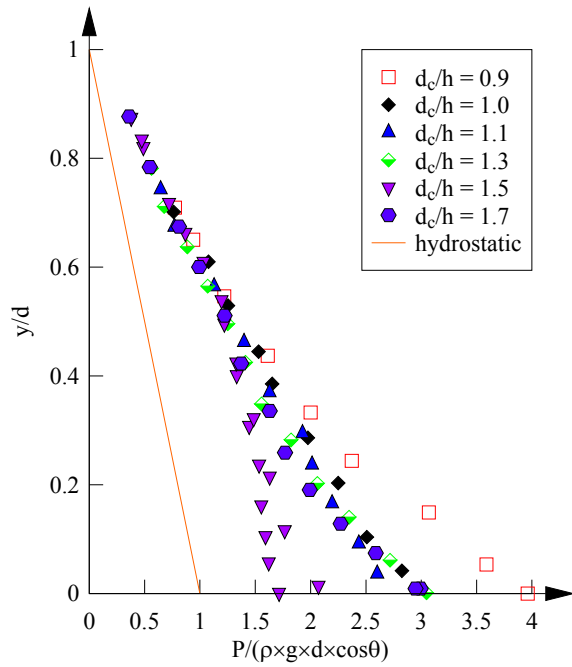
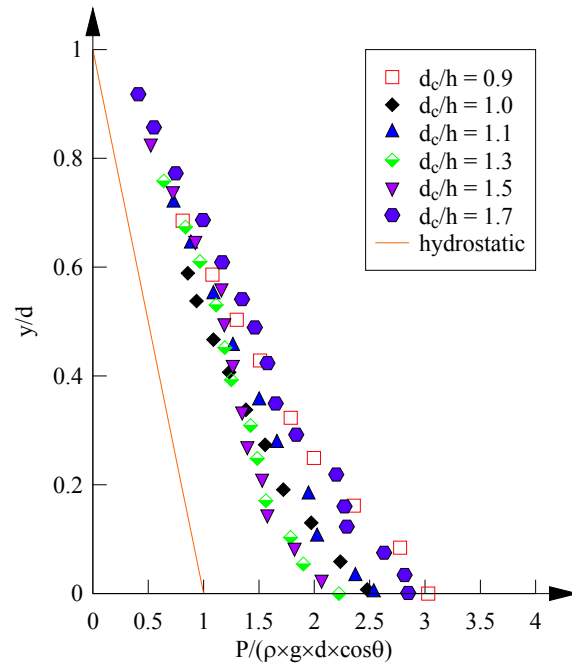


Fig. 5 - Dimensionless pressure distributions in skimming flows at locations immediately surrounding step edge 3

(A) $x/L_{cav} = -0.1$



(B) $x/L_{cav} = -0.05$



(C) Step edge 3: $x/L_{cav} = 0$

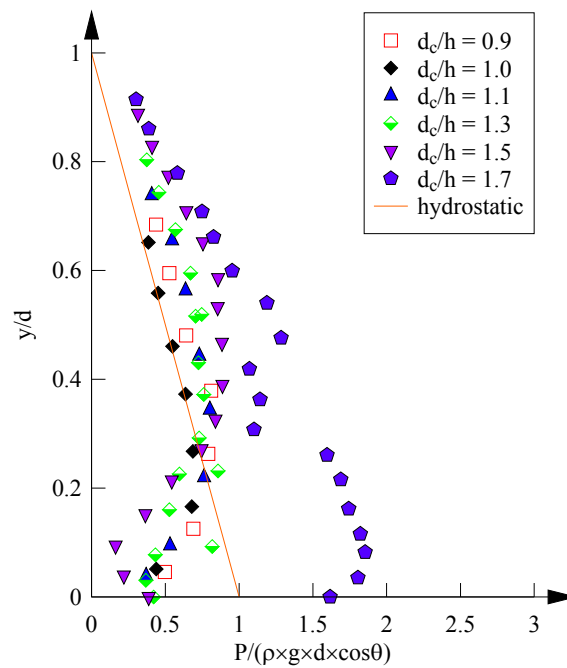
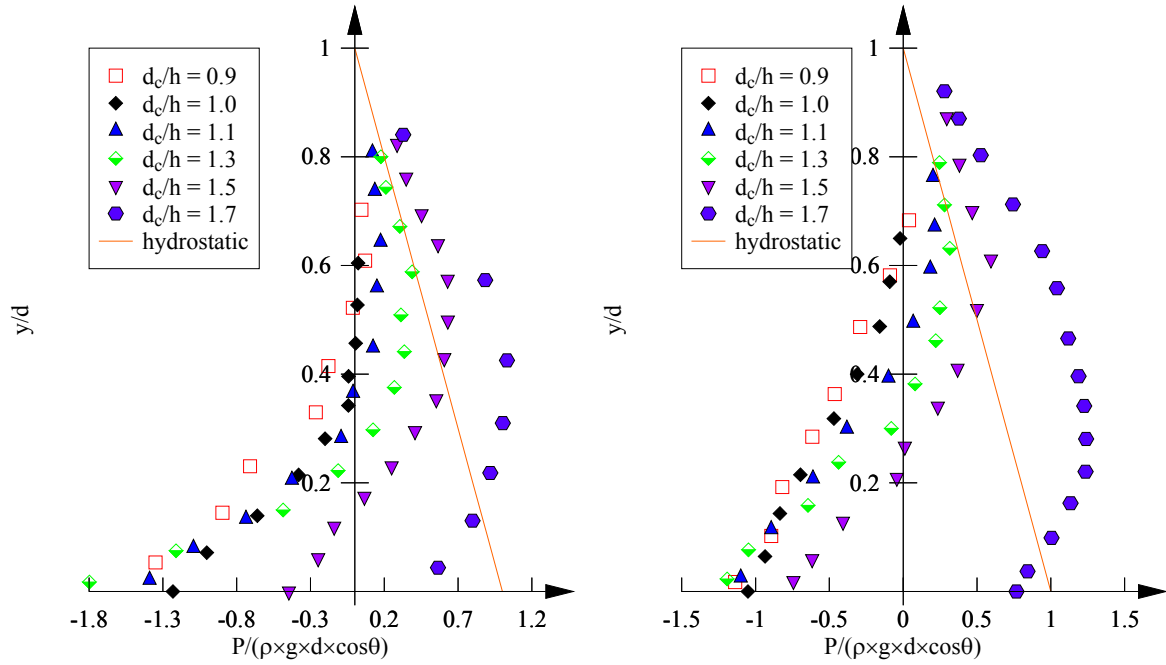


Fig. 5 - Dimensionless pressure distributions in skimming flows at locations immediately surrounding step edge 3

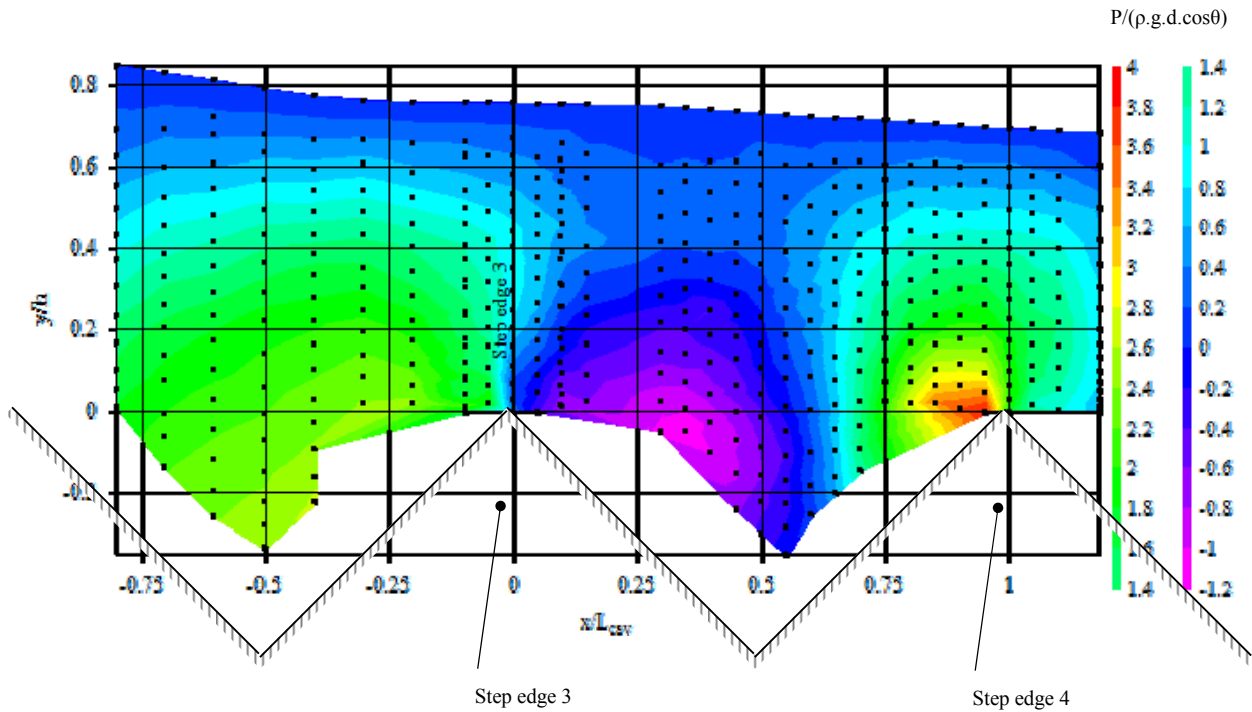
(D) $x/L_{cav} = +0.05$

(E) $x/L_{cav} = +0.1$



ZHANG, G., and CHANSON, H. (2016). "Hydraulics of the Developing Flow Region of Stepped Spillways. II: Pressure and Velocity Fields." *Journal of Hydraulic Engineering*, ASCE, Vol. 142, No. 7, 9 pages (DOI:10.1061/(ASCE)HY.1943-7900.0001136) (ISSN 0733-9429).

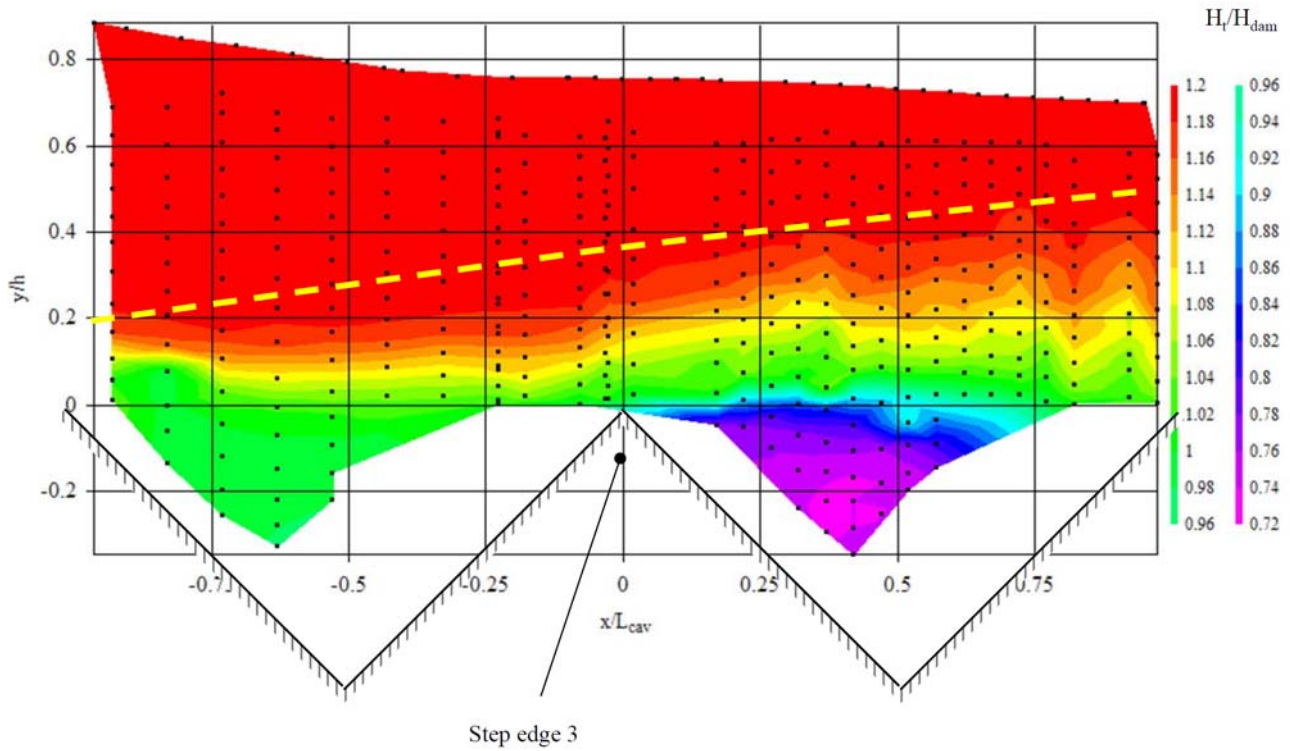
Fig. 6 - Dimensionless pressure field contour plot in skimming flow around step edge 3 - Flow conditions: $d_c/h = 1.5$, $h = 0.10$ m, Flow direction from left to right



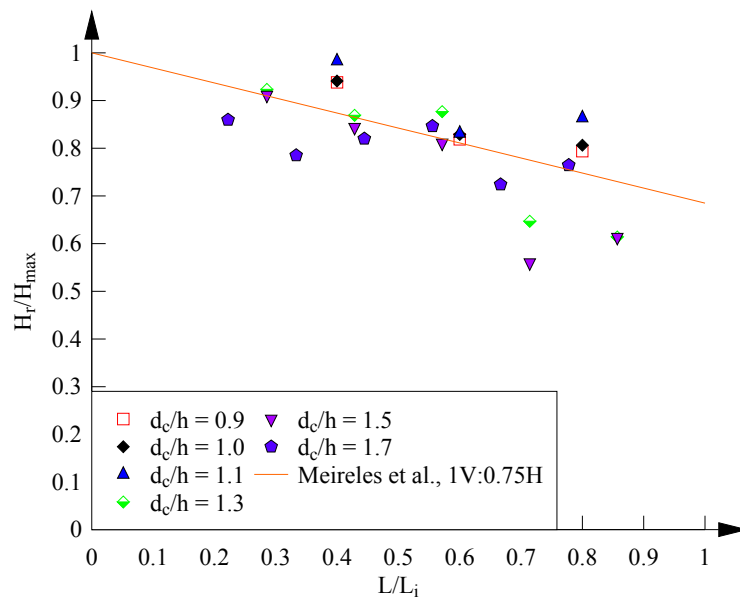
ZHANG, G., and CHANSON, H. (2016). "Hydraulics of the Developing Flow Region of Stepped Spillways. II: Pressure and Velocity Fields." *Journal of Hydraulic Engineering*, ASCE, Vol. 142, No. 7, 9 pages (DOI:10.1061/(ASCE)HY.1943-7900.0001136) (ISSN 0733-9429).

Fig. 7 - Total head distributions in the developing flow region of skimming flow

(A) Dimensionless total head distribution contours in skimming flows between step edges 2 and 4 for $d_c/h = 1.5$ - Yellow dashed line shows the outer edge of the boundary layer for that flow rate, Flow direction from left to right



(B) Longitudinal variation in dimensionless specific energy H_r/H_{max} in the developing flow region of skimming flows on a stepped spillway



ZHANG, G., and CHANSON, H. (2016). "Hydraulics of the Developing Flow Region of Stepped Spillways. II: Pressure and Velocity Fields." *Journal of Hydraulic Engineering*, ASCE, Vol. 142, No. 7, 9 pages (DOI:10.1061/(ASCE)HY.1943-7900.0001136) (ISSN 0733-9429).

Fig. 8 - Dimensionless boundary shear stress in the developing flow region of skimming flows on stepped spillways

